

# Kinetics of the Dispersion Copolymerization of Styrene and Butyl Acrylate

José M. Sáenz and José M. Asua\*

Grupo de Ingeniería Química, Departamento de Química Aplicada, Facultad de Ciencias Químicas, Universidad del País Vasco, Apdo. 1072, 20080 San Sebastián, Spain

Received January 29, 1998; Revised Manuscript Received May 8, 1998

**ABSTRACT:** The kinetics of the dispersion copolymerization of styrene and butyl acrylate in an ethanol–water medium was investigated in a batch stirred glass reactor. The effect of the stabilizer concentration, ethanol/water ratio, styrene/butyl acrylate ratio, temperature, and initiator concentration on the particle size distributions, conversion–time curves, and molecular weight distributions was investigated. It was found that the polymerization started in the continuous medium and, depending on the process conditions, the main polymerization locus shifted to the polymer particles. The more pronounced the shift, the higher  $\bar{M}_w$  and PI. The shift was more marked when the particles were small and when the solubility of the copolymer chains in the continuous medium was low. This solubility was the key factor in the process, as it also substantially affected the particle size.

## Introduction

Micron-size monodisperse polymer particles are used in a wide variety of scientific and technological applications.<sup>1,2</sup> These particles are difficult to obtain because their size lies between the size of the particles produced by conventional emulsion polymerization (0.05–0.7  $\mu\text{m}$ ) and by suspension polymerization (50–1000  $\mu\text{m}$ ). Although several techniques for the preparation of such micron-size monodisperse particles has been proposed,<sup>3–8</sup> dispersion polymerization is advantageous because micron-size monodisperse polymer particles can be prepared<sup>9,10</sup> in a single step. The production of micron-size monodisperse polymer particles requires a strict control of the nucleation, which should occur in a short period of time with neither posterior nucleation nor coagulation. This is not simple to achieve and most of the works reported in the literature were aimed at controlling the particle size distribution of the final dispersion.<sup>11–34</sup> Comparatively, the kinetics of particle growth has received less attention,<sup>9,10,35–50</sup> and the studies are mainly limited to homopolymerization.

In this work, the kinetics of the dispersion copolymerization of styrene and butyl acrylate in an ethanol–water medium was investigated considering both nucleation and particle growth. The effect of the stabilizer concentration, ethanol/water ratio, styrene/butyl acrylate ratio, temperature, and initiator concentration on the particle size distributions, conversion–time curves, and molecular weight distributions was investigated.

## Experimental Section

Styrene (St) and butyl acrylate (BuA) monomers were purified by washing with a 10% sodium hydroxide solution and then distilled under reduced pressure. Both monomers were stored at  $-18\text{ }^{\circ}\text{C}$  until used. Deionized water was used throughout the work. The other materials were used as received, including absolute ethanol (reagent grade, Panreac), poly(vinylpyrrolidone) (PVPK-30, PVPK-90, Janssen Chimica), azobis(isobutyronitrile) (AIBN, Fluka), and aerosol OT-100 (AOT-100: di-2-ethylhexyl ester of sodium sulfosuccinic acid, Cytec).

\* To whom correspondence should be addressed. Email: qppasgoj@sq.ehu.es

**Table 1. Recipe Representative of the Zone of Experimental Conditions<sup>a</sup> in Which Monodispersity Was Achieved**

total monomer (g)	32.13
St/BuA molar ratio	80.0/20.0 (100/0; 91.7/8.3; 80/20; 64.9/35.1; 55.2/44.8)
PVPK-30 (g)	4.284 (0.51; 0.56; 0.66; 0.81; 1.0; 2.0 wt %) <sup>b</sup>
AOT-100 (g)	1.071
AIBN (g)	0.643 (0.5; 1.0; 2.0 wt %) <sup>c</sup>
ethanol + water (g)	175.12
ethanol/water wt ratio	89/11 (78/22; 89/11; 100/0)
temperature ( $^{\circ}\text{C}$ )	65 (53; 60; 65; 69)

<sup>a</sup> Nitrogen purge. Propeller 300 rpm. <sup>b</sup> Based on total recipe. <sup>c</sup> Based on total monomer.

Polymerizations were carried out in a 0.45 L glass unbaffled jacketed reactor equipped with a reflux condenser, stainless steel stirrer, nitrogen inlet, and sampling device. Both the thermocouple and the tube for nitrogen purge and sampling were immersed in the reaction mixture. Special attention was paid to design a sealed system in order to avoid the entry of oxygen into the reactor during the polymerization.

Table 1 presents the standard recipe used in this work. This recipe resulted from preliminary experiments conducted to identify a range of experimental conditions in which fairly monodisperse micron-size dispersions could be produced. The effect of agitation on monomer conversion and particle size distribution was studied by using two stirrers (a propeller with diameter 3.5 cm and a disk turbine with diameter 4.5 cm and blade dimensions  $1.1 \times 1.2$  cm) and varying the agitation from 200 to 450 rpm (for the propeller). It was found that, within the experimental region, the agitation had no effect on the kinetics of the process. The polymerizations presented in this work were carried out using a propeller at 300 rpm. Based on this recipe, the effect of the stabilizer concentration, ethanol/water ratio, styrene/butyl acrylate ratio, temperature, and initiator concentration on the particle size distributions, conversion–time curves and molecular weight distributions was investigated. The values of these variables are given in parentheses in Table 1. The experimental procedure used in the reactions was as follows. Initially, water, some of the ethanol (generally, 116 g), PVPK-30 and AOT-100 were stirred (propeller, 300 rpm) in the reactor for 135 min at  $70\text{ }^{\circ}\text{C}$  under nitrogen purge (purity 99.999%, flow rate =  $5.8\text{ cm}^3/\text{min}$ ). Styrene and butyl acrylate were then added to the reactor. After 15 min, the reactor temperature was increased to  $72\text{ }^{\circ}\text{C}$ . Then, a solution of AIBN in the remaining ethanol was injected

into the reactor, decreasing the reactor temperature to the desired value (65 °C). The reaction time was measured once the solution of initiator was injected. A nitrogen purge was maintained during the reaction. Representative samples of the reaction medium were taken during the polymerizations and some drops of an aqueous solution of hydroquinone were added to the samples to short-stop the polymerization. The samples were dried in a vacuum at 45 °C and the overall conversion ( $x$ ) was determined gravimetrically. The molar ratio of the unreacted monomers in the system was measured by gas chromatography (Shimadzu GC-14A using a column 25QC5/BP20 1.0, Scientific Glass Engineering Inc.). The following oven temperature program was used: isothermal at 40 °C for 8 min, temperature ramp (40 °C/min) to 80 °C, isothermal at 80° for 5 min. The cumulative copolymer composition was calculated from the unreacted monomer ratio and the gravimetric overall conversion.

The particle size distributions (PSD) of the dispersions were measured without any washing (that may increase the monodispersity of the dispersions) using a disk centrifuge photo-sedimentometer (DCP, Brookhaven). The particle size distributions of some samples were also measured by transmission electron microscopy (TEM, H-7000 FA Hitachi). Number-average ( $\bar{d}_n$ ) and weight-average ( $\bar{d}_w$ ) diameters, coefficient of variation (CV), and polydispersity index ( $PDI = \bar{d}_w/\bar{d}_n$ ) were calculated from the particle size distribution. It has to be pointed out that DCP and TEM gave slightly, although significantly, different results. Thus, in a polymerization carried out using the recipe in Table 1 up to a conversion  $x = 0.65$ , a particle diameter  $\bar{d}_n = 2.2 \mu\text{m}$  and a polydispersity index  $PDI = 1.002$  were measured by DCP, whereas by TEM the same particle size but a  $PDI = 1.02$  was measured. The difference was due to the small (5.2% in number) and large (1.2% in number) offsize particles that were observed in the TEM but were undetected in the DCP. Thus the PDI obtained by TEM was, in general, higher than that measured by DCP. Offsize large particles in the monodisperse samples obtained by dispersion polymerization have been reported by Paine and McNulty<sup>15</sup> and Sáenz and Asua.<sup>28,32</sup> On the other hand, Sáenz and Asua<sup>32</sup> showed that offsize small particles appeared when the runs were carried out under isothermal conditions, but these small particles were avoided when the temperature was raised after the onset of the nucleation.

The molecular weight distributions (MWD) were obtained by gel permeation chromatography (GPC) using a Waters 410 equipment with a dual detector: refractometer and viscometer (Viscotek, model 250). Three columns in series were used (styragel HR6, Ultrastrygel 10<sup>4</sup> Å, and styragel HR2; Waters). The detector and columns were at 40 °C. Distilled tetrahydrofuran (THF) was used as solvent (flow rate = 1.0 mL/min.) The calibration was carried out using monodisperse polystyrene standards (Polymer Laboratories). Number-average ( $\bar{M}_n$ ) and weight-average ( $\bar{M}_w$ ) molecular weights, and polydispersity index ( $PI = \bar{M}_w/\bar{M}_n$ ) were calculated from the MWD.

## Results and Discussion

**Effect of the Stabilizer Concentration.** The study of the effect of the stabilizer concentration was carried out using the recipe shown in Table 1. The PVPK-30 concentration was varied between 2 and 0.51 wt %, the concentration at which the dispersion coagulated. Table 2 shows that the particle size increased when the stabilizer concentration decreased. This is in agreement with the results obtained by Sáenz and Asua<sup>32</sup> for the dispersion copolymerization of styrene and butyl acrylate in an ethanol–water medium carried out in a bottle. Similar results have been reported in the literature for the dispersion polymerization of styrene<sup>11,22,41,45,46</sup> and methyl methacrylate<sup>16,18,20,24</sup> in polar media.

The formation of particles in dispersion polymerization is believed to occur in several steps. First, polymer chains are formed in the continuous phase through

**Table 2. Effect of the Stabilizer Concentration: (i) on  $\bar{d}_n$  and PDI and (ii) on  $\bar{M}_w$  and PI**

run <sup>a</sup>	[PVPK-30] <sup>b</sup>	$t_p$ (h) <sup>c</sup>	$x$	$\bar{d}_n$ ( $\mu\text{m}$ ) <sup>d</sup>	PDI <sup>d</sup>	$\bar{M}_w$	PI
S1bis	2.0	27.5	0.98	2.6	1.005	50 000	3.0
S12	1.0	27.2	1.00	3.0	1.003	39 700	3.6
S13	0.81	28.2	0.97	3.7	1.005		
S14	0.66	23.0	0.97	3.5	1.008		
S15	0.56	27.5	0.91	5.6	1.6	26 300	2.1
S16	0.51	10.0	0.77	3.8 <sup>e</sup>	1.11		
S16	0.51		0.77 > $x$ > 1	coagulum			

<sup>a</sup> These runs are based on the standard run shown in Table 1, changing only the stabilizer concentration. <sup>b</sup> PVPK-30 stabilizer concentration (wt % based on total recipe). <sup>c</sup> Polymerization time. <sup>d</sup> Measured by DCP. <sup>e</sup> Extrapolated to  $x = 1$ .

polymerization initiated by the decomposition of the initiator. As the composition of the continuous phase is chosen in such a way the polymer is not soluble in the medium, precipitation of polymer chains occurs and nuclei are formed. When homopolymers as PVPK-30 are used as stabilizers, the stabilizing efficiency of the unmodified PVPK-30 is rather poor as it is soluble in the medium, but its stabilizing power increases sharply after suffering a grafting reaction. The PVPK-30 molecules with a grafted chain of copolymer St–BuA are very efficient stabilizers because one of the blocks is soluble in the medium and the other is insoluble and of the same nature as the polymer in the particles. In addition, for a given poly(vinylpyrrolidone), the efficiency depends on the length of the grafted chains. The shorter the chain, the more soluble in the medium the whole molecule and hence the weaker its stability power.

Therefore, at the beginning of the process, the total area of the nuclei formed exceeds the area that can be stabilized by the grafted stabilizer (and the small contribution of the ungrafted one) and the nuclei coagulate. On the other hand, as process time increases, the amount of grafted stabilizer increases (according to the grafting kinetics) and the grafted molecules move to the interfacial area polymer-continuous medium. Consequently, stable particles appear in the system. These stable particles act as a sink for both polymer chains growing in the continuous medium and nuclei, and hence when the number of stable polymer particles is high enough, the probability of new nucleations approaches zero and this is the end of the nucleation. Clearly, the higher the concentration of PVPK-30 the more grafted molecules will be formed and the larger the interfacial area that they will be able to stabilize, namely, the smaller the particle size, as was found experimentally (Table 2).

Table 2 also shows that the particle size obtained in run S16 was smaller than the particle size obtained in run S15, although a lower amount of stabilizer was used in the run. This result may be attributed to the low reproducibility of the process when the amount of PVPK-30 was reduced below a critical value and uncontrolled particle coalescence process occurred. This coalescence is also responsible for the broadening of the PSDs in runs S15 and S16, as a matter of fact, run S16 coagulated sometime after  $x = 0.77$ .

Figure 1 presents the evolution of the overall conversion for the different stabilizer concentrations. The period without experimental points corresponds to night-time. From these curves, the polymerization rate,  $R_p$ , was calculated by fitting the overall conversion

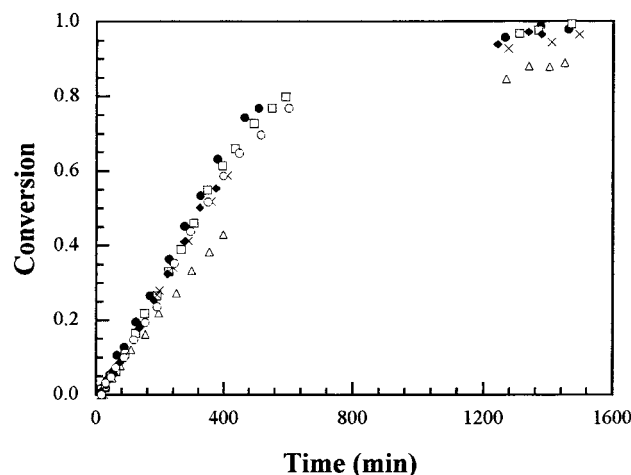


**Figure 1.** Effect of the stabilizer concentration on the overall conversion. Legend: (●) run S1bis, [PVPK-30] = 2.0 wt %; (□) S12, [PVPK-30] = 1.0 wt %; (×) S13, [PVPK-30] = 0.81 wt %; (◆) S14, [PVPK-30] = 0.66 wt %; (△) S15, [PVPK-30] = 0.56 wt %; (○) S16, [PVPK-30] = 0.51 wt % based on total recipe.

versus time data to a polynomial and differentiating the polynomial (Figure 2). It can be seen that, although the initial polymerization rate is not affected by the stabilizer concentration, the evolution of  $R_p$  can be very different. In some runs,  $R_p$  first increased and, after going through a maximum, decreased in the second part of the process. On the other hand, in run S15, the polymerization rate decreased continuously. Similar results were obtained by Lu et al.<sup>41,43</sup> and Tuncel et al.<sup>46</sup> for the dispersion polymerization of styrene in ethanol. A possible explanation of this behavior is as follows. At the beginning of the process, polymerization occurs mostly in the continuous phase, in a similar way to solution polymerization, and as temperature, concentration of initiator, and concentration of monomer were the same in all experiments, the initial polymerization rate was also similar. The polymerization rate in solution referred to the whole reactor (in g/h to compare with Figure 2) can be estimated as follows:

$$R_p = \{(k_{p11}P_1 + k_{p21}P_2)M_1P_{m1} + (k_{p12}P_1 + k_{p22}P_2)M_2P_{m2}\} \left[ \frac{fk_1[I]}{k_t} \right]^{0.5} 3600$$

where  $k_{p_{ij}}$  are the propagation rate constants,  $P_i$  is the probability of having a growing chain with ultimate unit of type  $i$ ,  $M_i$  is the amount (moles) of monomer  $i$  in the reactor,  $P_{mi}$  is the molecular weight of the monomer  $i$ ,  $f$  is the efficiency factor of the initiator,  $k_1$  is the rate constant for initiator decomposition,  $[I]$  is the concentration of the initiator, and  $k_t$  is the average termination rate constant. Using the values of the parameters in Table 3,  $R_p = 2.67$  g/h, which compares well with the initial polymerization rates reported in Figure 2.

Later, in the runs in which, as a result of the large amount of stabilizer used, the number of particles was high (particle size relatively small), the main polymerization locus shifted from the continuous medium to the polymer particles. Due to the high internal viscosity of the particles, the termination rate constant was low, yielding a high concentration of radicals, and hence a  $R_p$  higher than that of the continuous medium. It is worth pointing out that the continuous increase of  $R_p$  is not the result of a long nucleation period but that of

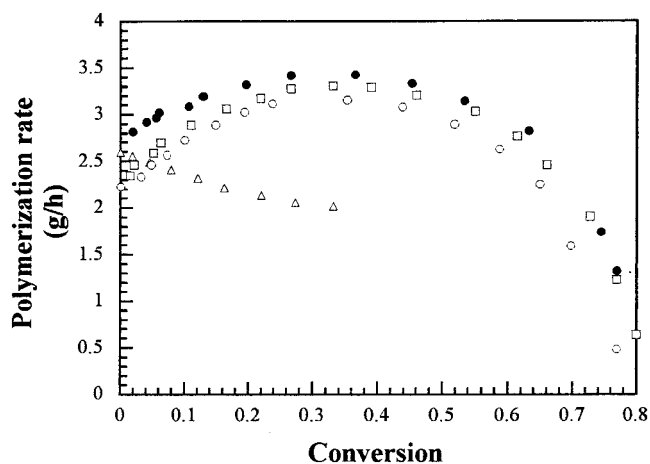


**Figure 2.** Effect of the stabilizer concentration on the polymerization rate. Legend: (●) run S1bis, [PVPK-30] = 2.0 wt %; (□) S12, [PVPK-30] = 1.0 wt %; (△) S15, [PVPK-30] = 0.56 wt %; (○) S16, [PVPK-30] = 0.51 wt % based on total recipe.

**Table 3. Values of the Parameters**

$k_{p11} = 406$ (L/mol s) <sup>51</sup>	$k_{t11} = 0.76 \times 10^8$ (L/mol s) <sup>52</sup>
$k_{p22} = 36\,960$ (L/mol s) <sup>51</sup>	$k_{t22} = 0.85 \times 10^9$ (L/mol s) <sup>52</sup>
$r_1 = 0.95^{51}$	$r_2 = 0.18^{51}$
$f = 0.5$	$k_1 = 1.9 \times 10^{-5}$ (s <sup>-1</sup> ) <sup>52</sup>

**Table 4. Evolution of  $\bar{M}_w$  and PI during the Run S1bis**

$x$	$\bar{M}_w$	PI
0.05	24 900	2.4
0.09	24 500	1.9
0.46	39 900	2.2
0.73	50 600	3.1
1.00	50 000	3.0

the increase of the volume of the polymer particles due to the particle growth. The hypothesis of a shift of the polymerization locus is also supported by the evolution of  $\bar{M}_w$  in run S1bis presented in Table 4. It can be seen that the molecular weight increased during the process, in agreement with a shift of the polymerization locus from the continuous phase to the polymer particles where a higher molecular weight was produced as a result of the gel effect. In addition, Table 4 shows that PI also increases during the process due to the formation of polymer in different environments. In run S15, the number of particles was much lower than in the other runs; therefore, the overall rate of radical absorption from the continuous medium was rather low and, during the whole process, the main polymerization locus was the continuous medium. This resulted in a continuously decreasing  $R_p$  typical of solution polymerization. Table 2 shows that both  $\bar{M}_w$  and the polydispersity index, PI, in run S15 were significantly lower than in the other runs.

**Effect of the Ethanol/Water Ratio.** Figure 3 presents the effect of the composition of the continuous phase (ethanol/water weight ratio) on the evolution of the polymerization rate during the process. It can be seen that very different evolutions were obtained. When a high fraction of water was used (22% in run S21), the polymerization rate first increased and, after going through a maximum, decreased in the final part of the process. The maximum was less pronounced when the fraction of water was reduced to 11% (run S1bis) and completely disappeared when pure ethanol was used as the continuous phase. On the other hand, all reactions had the same initial polymerization rate.



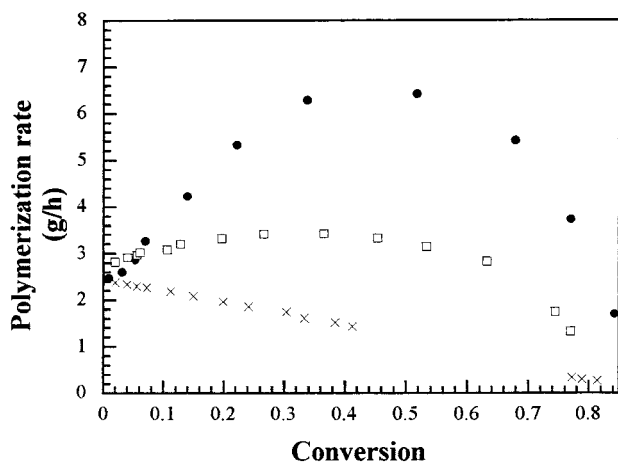


**Figure 3.** Effect of the EtOH/H<sub>2</sub>O ratio on the polymerization rate. Legend: (●) run S21, EtOH/H<sub>2</sub>O wt ratio = 78.0/22.0; (□) S1bis, EtOH/H<sub>2</sub>O = 89.0/11.0; (×) S22, EtOH/H<sub>2</sub>O = 100/0.

**Table 5.** Effect of the EtOH/H<sub>2</sub>O Ratio: (i) on  $\bar{d}_n$  and PDI and (ii) on  $\bar{M}_w$  and PI

run <sup>a</sup>	EtOH/H <sub>2</sub> O <sup>b</sup>	$x^c$	$\bar{d}_n$ (μm) <sup>d</sup>	PDI <sup>d</sup>	$\bar{M}_w$	PI
S21	78.0/22.0	1.00	1.5	1.03	80 100	6.3
S1bis	89.0/11.0	0.98	2.6	1.005	50 000	3.0
S22	100/0	0.81	4.0	1.95	17 700	3.0

<sup>a</sup> These runs are based on the standard run shown in Table 1, changing only the EtOH/H<sub>2</sub>O weight ratio. <sup>b</sup> EtOH/H<sub>2</sub>O weight ratio. <sup>c</sup> Conversion at a polymerization time of 28 h. <sup>d</sup> Measured by DCP.

The particle size,  $\bar{M}_w$ , and PI for the final dispersion of these reactions are presented in Table 5. It can be seen that the particle size increased and both  $\bar{M}_w$  and PI decreased with the ethanol content of the continuous medium. In addition, a very broad particle size distribution was obtained when pure ethanol was used.

The key factor behind these results was the solubility of the St–BuA copolymer in the continuous medium. Effects of the solvency of the medium on the kinetics of the dispersion polymerization of styrene<sup>10,17,22,38,46</sup> and methyl methacrylate<sup>18,20</sup> in polar media have been reported. The higher the amount of ethanol in the continuous medium, the more soluble was the copolymer. Therefore, the adsorption equilibrium of the grafted stabilizer shifted toward a lower adsorption, and hence less surface could be stabilized with a given amount of stabilizer. This resulted in an increase of the particle size as the continuous medium became richer in ethanol. It can be argued that this effect can somehow be counteracted by the higher extent of the grafting reactions that resulted from the higher concentration of radicals in the continuous medium (see below). However, the experimental results showed that this effect, if present, was overridden by the shift of the adsorption equilibrium.

As in the case of the effect of stabilizer concentration, the differences in particle sizes may account for some of the observed behavior of the polymerization rate. However, comparison between Figures 2 and 3 shows that the change in  $R_p$  was substantially more pronounced when the composition of the continuous medium was changed. The reason for this additional effect on  $R_p$  was the influence of the composition of the continuous medium on the critical length for precipitation of the copolymer growing chains. The more hydrophilic the continuous medium, the shorter the critical

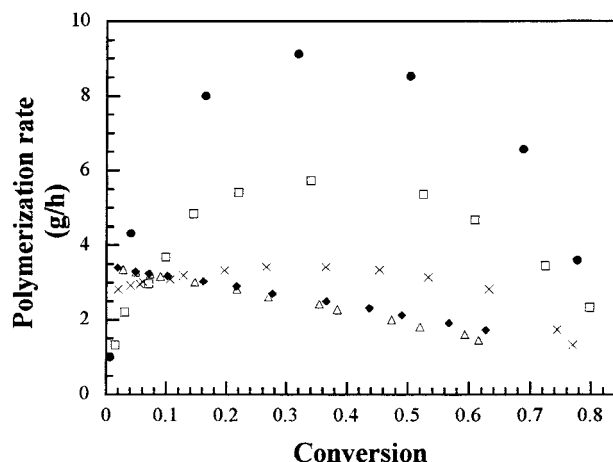


**Figure 4.** Effect of the St/BuA ratio on the evolution of the polymerization rate. Legend: (●) run S17, St/BuA molar ratio = 100/0; (□) S18, St/BuA = 91.7/8.3; (×) S1bis, St/BuA = 80.0/20.0; (◆) S19, St/BuA = 64.9/35.1; (△) S20, St/ABu = 55.2/44.8.

length and the less important the polymerization in the continuous medium. Therefore, when a water-rich continuous medium was used, the polymerization in the polymer particles was more important because (1) the particles were small (and hence a large total number of particles was present, which gave a high rate of radical absorption) and (2) the critical length for precipitation was short (which reduced the polymerization in the continuous medium). On the other hand, an ethanol-rich continuous medium led to large particles (low efficiency for capture of radicals) and long radicals in the continuous medium (increase of the solution-like polymerization). In agreement with these arguments,  $\bar{M}_w$  and PI also decreased with the increase of the ethanol content.

Furthermore, Table 5 shows that the ethanol/water ratio was critical for the polydispersity of the particle size distribution. In the experimental region studied, the ethanol/water ratio of 89/11 was the best to obtain a narrow particle size distribution (run S1bis). When an ethanol/water ratio of 78/22 was used instead, the particle size distribution broadened (run S21). On the other hand, when a ethanol/water ratio of 100/0 was used, a highly polydisperse dispersion was obtained (run S22).

**Effect of the Styrene/Butyl Acrylate Ratio.** The effect of styrene and butyl acrylate in the system was studied by changing the ratio between the two monomers in the standard recipe shown in Table 1. Figure 4 presents the effect of the monomer ratio on the polymerization rate. This figure presents some interesting results. At the beginning of the process, the higher the content of BuA of the monomer mixture the higher the polymerization rate. However, later in the process, the polymerization rate of the BuA-rich monomer mixtures decreased continuously, presenting a solution-like behavior, whereas the polymerization rates of the St-rich monomer mixtures increased up to a maximum and then decreased. In addition, the maximum was more pronounced as the St content increased.

Table 6 presents the effect of the monomer mixture composition on the particle size, PDI,  $\bar{M}_w$ , and PI. It can be seen that the particle size increased with the BuA content, whereas  $\bar{M}_w$  and PI decreased. Ober and Lok<sup>13</sup> also observed that the particle size increased when the styrene/*n*-butyl methacrylate ratio decreased in the

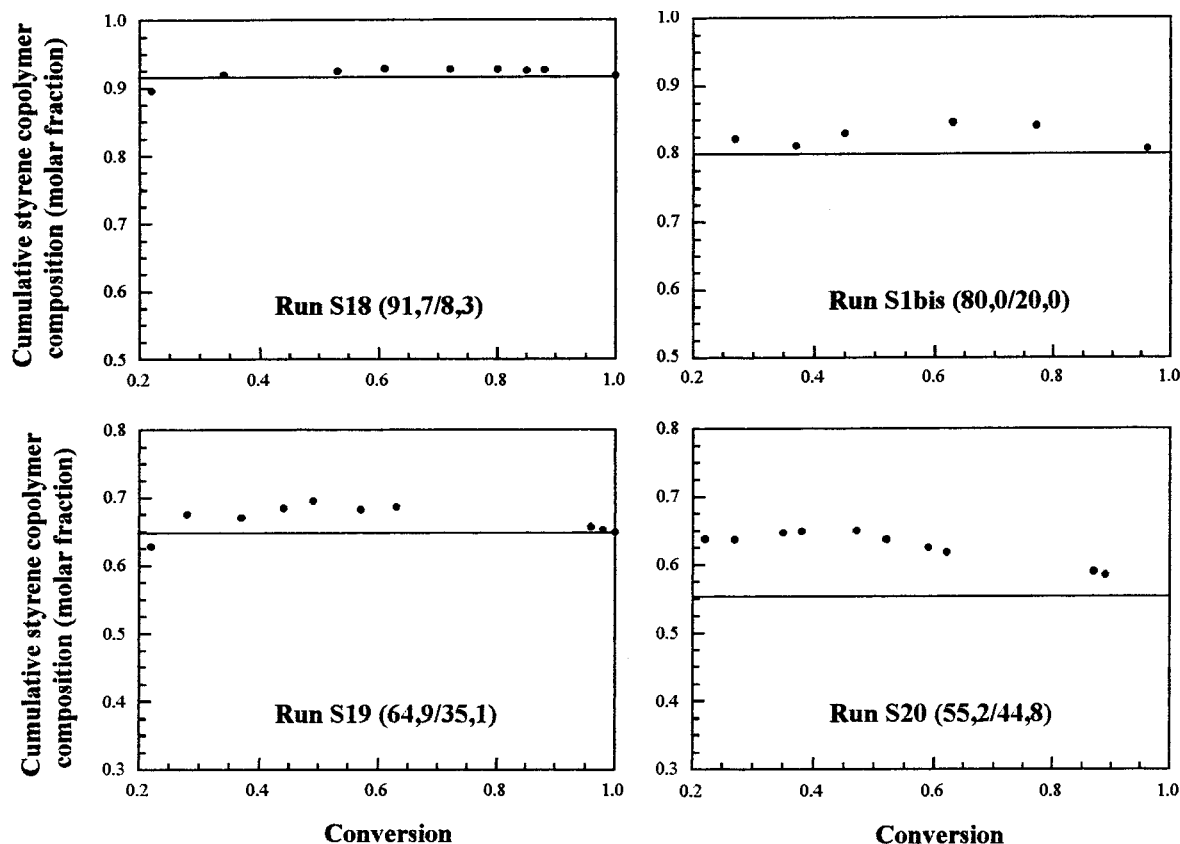


**Figure 5.** Evolution of the cumulative styrene copolymer composition during the reactions carried out with different St/BuA ratios. The horizontal line represents the initial monomer molar ratio.

**Table 6.** Effect of the St/BuA Ratio: (i) on  $\bar{d}_n$  and PDI and (ii) on  $\bar{M}_w$  and PI

run <sup>a</sup>	St/BuA <sup>b</sup>	$x^c$	$\bar{d}_n$ ( $\mu\text{m}$ ) <sup>d</sup>	PDI <sup>d</sup>	$\bar{M}_w$	PI
S17	100/0	1.00	1.6	1.002	199 500	11.2
S18	91.7/8.3	1.00	2.1	1.002	100 300	6.2
S1bis	80.0/20.0	0.98	2.6	1.005	50 000	3.0
S19	64.9/35.1	1.00	3.5	1.3	26 300	2.6
S20	55.2/44.8	0.91	4.9	1.1	24 500	1.9

<sup>a</sup> These runs are based on the standard run shown in Table 1, changing only the St/BuA ratio. <sup>b</sup> St/BuA molar ratio. <sup>c</sup> Conversion at a polymerization time of 27.5 h. <sup>d</sup> Measured by DCP.

dispersion copolymerization of these two monomers in an ethanol–water medium. Figure 5 presents the evolution of the copolymer composition during the process for the different monomer compositions. The St/(St + BuA) monomer ratio used in each run is given by a continuous line. The data are for conversions higher than  $x = 0.2$  because for lower conversions, the compositions calculated using GC and gravimetry measurements involved significant errors. It can be seen that either a negligible or a very moderate copolymer composition drift was observed.

At the beginning of the process, polymerization occurred in the continuous medium and  $R_p$  increased with the BuA content simply because of the higher  $k_p/k_t$  ratio for this monomer as compared with styrene ( $k_p$ : propagation rate constant;  $k_t$ : termination rate constant). On the other hand, the posterior behavior of  $R_p$  was determined by the solubility of the copolymer chains in the continuous medium. The solubility of the copolymer in the ethanol/water mixture increased as the BuA content increased (actually, p-BuA is soluble in the ethanol/water mixture). Therefore, the increase in BuA content for a given ethanol/water mixture has the same

effects as increasing the ethanol content of the continuous medium for a given monomer composition: an increase in particle size, a greater importance of the polymerization in the continuous medium, and a decrease of the average molecular weights and the broadness of the MWD. Table 6 shows that when the styrene/butyl acrylate ratio was lower than a certain value, polydisperse dispersions were obtained (runs S19, St/BuA = 64.9/35.1, and S20, St/BuA = 55.2/44.8).

Simple calculations using the reactivity ratios ( $r_{\text{St}} = 0.95$ ,  $r_{\text{BuA}} = 0.18$ )<sup>51</sup> show that the azeotropic composition assuming equal distribution of both monomers between the phases was 0.84/0.16, which agrees rather well with the results in Figure 5.

**Effect of the Temperature.** The effect of the temperature was studied using the recipe given in Table 1. Four isothermal runs (S7, S8, S1, and S9: 53, 60, 65, and 69 °C, respectively) as well as one nonisothermal polymerization (run S10) were carried out. Table 7 shows the particle size and PDIs of the dispersions obtained in these runs. The PSDs were measured by disk centrifuge photosedimentometer and transmission electron microscopy. The number-average particle diameters extrapolated to conversion  $x = 1$  show that, in the isothermal polymerizations, the particle diameter increased with the reaction temperature. Similar results have been reported for the dispersion polymerization of styrene<sup>17,34,37,41</sup> and methyl methacrylate<sup>20</sup> in polar media. An increase of the reaction temperature leads to an increase of the rate of generation of radicals and perhaps of the solubility of the oligomer chains and grafted stabilizer and to a decrease of the length of the copolymer chains. The last two factors result in a decrease of the stabilizing power of the grafted poly-

**Table 7. Effect of the Reaction Temperature on  $\bar{d}_n$  and PDI**

run <sup>a</sup>	temp (°C)	$t_p$ (h) <sup>b</sup>	$x$	$\bar{d}_n$ ( $\mu\text{m}$ ) <sup>c</sup>	PDI <sup>c</sup>	$\bar{d}_n$ ( $\mu\text{m}$ ) <sup>d</sup>	PDI <sup>d</sup>	small particles <sup>e</sup>	$\bar{d}_n$ ( $x = 1$ ) <sup>f</sup> ( $\mu\text{m}$ ) <sup>c</sup>
S7	53	27.5	0.95	1.6	1.04	1.7	1.04	12	1.6
S8	60	5.8	0.46	1.5	1.001	1.5	1.02	4	1.9
S1	65	6.4	0.65	2.2	1.002	2.2	1.02	5	2.5
S9	69	6.4	0.72	2.7	1.03	2.7	1.04	13	3.1
S10	53–70	27.3	0.99	1.7	1.002	1.8	1.003	0	1.7

<sup>a</sup> These runs are based on the standard run shown in Table 1, changing only the reaction temperature. <sup>b</sup> Polymerization time. <sup>c</sup> Measured by DCP. <sup>d</sup> Measured by TEM. <sup>e</sup> Number percent based on the total number of particles (obtained by TEM). <sup>f</sup> Number average particle diameter extrapolated to conversion  $x = 1$  (using the data obtained by DCP).

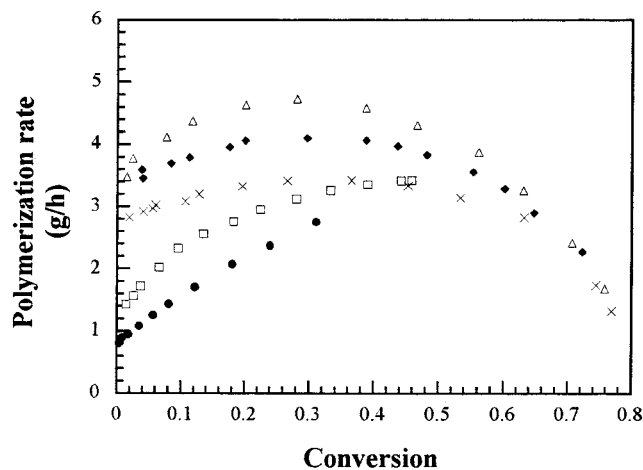


**Figure 6.** Effect of the temperature on the evolution of the polymerization rate. Legend: (●) run S7, 53 °C; (□) S8, 60 °C; (×) S1bis, 65 °C; (◆) S9, 69 °C; (△) S10, from 53 to 70 °C.

**Table 8. Effect of the Reaction Temperature on  $\bar{M}_w$  and PI**

run	temp (°C)	$\bar{M}_w$		
		$x \approx 0.5$	$x \approx 0.7$	$x \approx 1.0$
S7	53	206 900 (3.6) <sup>a</sup>		207 300 (5.4)
S8	60	64 500 (2.4)		
S1bis	65	39 900 (2.2)	50 600 (3.1)	50 000 (3.0)
S9	69	24 700 (2.2)	27 200 (2.1)	
S10	53–70			31 300 (2.8)

<sup>a</sup> The number in parentheses is the polydispersity index (PI) of the MWD.

(vinylpyrrolidone). In addition, the shorter the copolymer chains, the lower the rate for nuclei formation and the lower the number of particles (larger size). Figure 6 presents the polymerization rates obtained in the isothermal experiments. It can be seen that, as expected, the polymerization rate increased with temperature. However, the relative increase of  $R_p$  during each run decreased with temperature. This means that the shift of the polymerization locus is more marked at low temperature. This may be due to (i) the smaller particle size and (ii) shorter chain lengths obtained at higher temperatures, which, combined with a higher solubility, increased the importance of the polymerization in the continuous phase. An additional effect may be the fact that the gel effect is more severe at low temperatures,<sup>53</sup> and hence the difference in radical concentration between the polymer particles and the continuous phase increased as the temperature decreased. Table 8 shows that  $\bar{M}_w$  and PI of these dispersions increased when the temperature decreased. The variation of  $\bar{M}_w$  is mainly caused by the effect of the temperature on the bulk polymerization kinetics, and the higher values of PI at low temperatures were due to the more pronounced shift of the polymerization locus.

**Table 9. Effect of the Initiator Concentration: (i) on  $\bar{d}_n$  and PDI and (ii) on  $\bar{M}_w$  and PI**

run <sup>a</sup>	[AIBN] <sup>b</sup>	$x^c$	$\bar{d}_n$ ( $\mu\text{m}$ ) <sup>d</sup>	PDI <sup>d</sup>	$\bar{M}_w$	PI
S2bis	0.5	0.92	1.6	1.01	170 900	4.1
S11	1.0	1.00	2.1	1.003	84 700	4.0
S1bis	2.0	0.98	2.6	1.005	50 000	3.0

<sup>a</sup> These runs are based on the standard run shown in Table 1, changing only the initiator concentration. <sup>b</sup> AIBN initiator concentration (wt % based on total monomer). <sup>c</sup> Conversion at a polymerization time of 24 h. <sup>d</sup> Measured by DCP.

On the other hand, Table 7 shows that a population of small particles was detected by TEM in the four runs carried out under isothermal conditions (S7, S8, S1, and S9). These small particles were not detected by DCP in runs S8 and S1 due to their low concentration, and hence the PDI obtained by TEM was higher than that obtained by DCP. Sáenz and Asua<sup>32</sup> showed that small particles were avoided when the temperature was raised after the onset of the nucleation. Thus, run S10 was carried out by starting the polymerization at 53 °C and increasing the temperature to 70 °C once the reaction medium became opalescent. Table 7 shows that no small particles were observed by TEM in run S10, yielding a highly monodisperse PSD.

**Effect of the Initiator Concentration.** The effect of the AIBN initiator concentration was studied using the standard recipe shown in Table 1. Three runs (S1bis, S11, and S2bis) were carried out using three different AIBN initiator concentrations (2%, 1%, and 0.5 wt % based on total monomer). Table 9 shows that the particle size increased when the initiator concentration was increased. Monodisperse particle size distributions were obtained in runs S1bis, S11, and S2bis. The increase in the particle size provoked by the increase in the initiator concentration has also been reported in the literature for the dispersion polymerization of styrene<sup>11,17,22,37,41,45,47</sup> and methyl methacrylate<sup>16,18,20</sup> in polar media. However, as pointed out by Sudol,<sup>2</sup> this result is not universal as the opposite trend has been reported for the dispersion polymerization of BuA. According to the results shown in Table 9, the number-average particle diameter depends on the initiator concentration to the power 0.35. This value is in agreement with the dependence reported in the literature for the effect of the initiator concentration in the dispersion polymerization of styrene in polar media.<sup>11,41,45,47</sup> Several and sometimes conflicting explanations for the effect of the initiator concentration on the particle size have been given (see ref 2 for a discussion on this subject). The most commonly offered is that the increase of the initiator concentration decreases the length of the copolymer chains and therefore both the stabilizing ability of the grafted stabilizer and the rate of nuclei formation decrease leading to a lower number of particles of larger size.



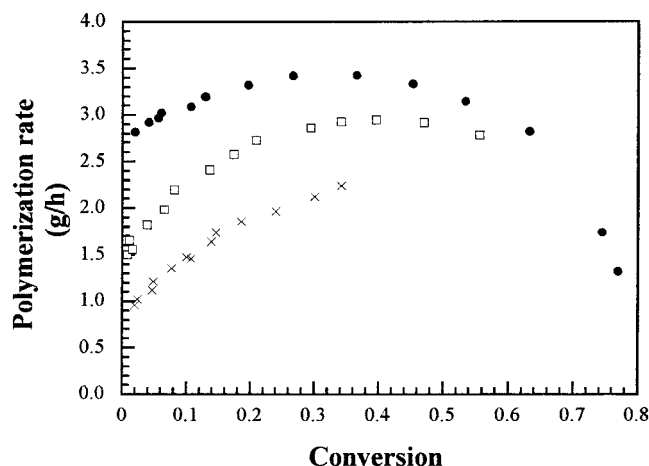


**Figure 7.** Effect of the initiator concentration on the evolution of the polymerization rate. Legend: (●) run S1bis, [AIBN] = 2.0 wt %; (□) S11, [AIBN] = 1.0 wt %; (×) S2bis, [AIBN] = 0.5 wt % based on total monomer

Figure 7 shows the effect of initiator concentration on the evolution of the polymerization rate during the reaction. As expected,  $R_p$  increased with the initiator concentration. In addition, the maximum of  $R_p$  was relatively more pronounced at low initiator concentrations, probably due to the smaller particle size. Table 9 also shows that, as is typical of bulk and solution polymerization, the molecular weight decreased when the initiator concentration increased. The polydispersity index did not vary substantially.

## Conclusions

The kinetics of the dispersion copolymerization of styrene and butyl acrylate in an ethanol–water medium was investigated in a batch-stirred glass reactor. Preliminary experiments were conducted to identify a range of experimental conditions in which fairly monodisperse micron-size dispersions could be produced. The effect of the stabilizer concentration ethanol/water ratio, styrene/butyl acrylate ratio, stabilizer concentration, temperature, and initiator concentration on the particle size distributions, conversion–time curves, and molecular weight distributions was investigated.

It was found that the polymerization started in the continuous medium and, depending on the process conditions, the main polymerization locus shifted to the polymer particles. A consequence was that the more pronounced the shift the higher  $\bar{M}_w$  and PI. The shift was more marked when the size of the particles was small and when the solubility of the copolymer chains in the continuous medium was low. This solubility was the key factor in the process, as it also affected substantially the particle size. The higher the solubility, the larger the particle size because (i) the adsorption equilibrium of the grafted stabilizer shifted toward a lower adsorption, hence decreasing the area that can be stabilized, and (ii) the critical length for oligomer precipitation increased and consequently fewer nuclei were formed. As a result, the particle size increased with both the ethanol content of the continuous medium and the BuA content of the monomer mixture. The particle size also increased when the amount of stabilizer decreased, the temperature increased, and the initiator concentration increased. The last two variables affected the particle size by reducing the lengths of the copolymer chains produced.

**Acknowledgment.** The financial support by the Universidad del País Vasco (U.P.V./E.H.U.) under Grant UPV 221.215-EB020/92 is greatly appreciated. J.M.S. acknowledges the fellowship from the Basque Government.

## References and Notes

- (1) Ugelstad, J.; Berge, A.; Ellingsen, T.; Schmid, R.; Nilsen, T.-N.; Mork, P. C.; Stenstad, P.; Hornes, E.; Olsvik, O. *Prog. Polym. Sci.* **1992**, *17*, 87.
- (2) Sudol, E. D. In *Polymeric Dispersions: Principles and Applications*; Asua, J. M., Ed.; Kluwer Academic Publishers: Dordrecht, The Netherlands, 1997.
- (3) Vanderhoff, J. V.; El-Aasser, M. S.; Micale, F. J.; Sudol, E. D.; Tseng, C. M.; Silwanowicz, A.; Kornfeld, D. M.; Vicente, F. A. *J. Dispersion Sci. Technol.* **1984**, *5*, 231.
- (4) Ugelstad, J.; Mork, P. C.; Kaggerud, K. H.; Ellingsen, T.; Berge, A. *Adv. Colloid Interface Sci.* **1980**, *13*, 101.
- (5) Ugelstad, J.; Mork, P. C.; Berge, A.; Ellingsen, T.; Khan, A. A. In *Emulsion Polymerization*; Piirma, I., Ed.; Academic Press: New York, 1982; p 383.
- (6) Omi, S.; Katami, K.; Yamamoto, A.; Iso, M. *J. Appl. Polym. Sci.* **1994**, *51*, 1.
- (7) Kamiyama, M.; Koyama, K.; Matsuda, H.; Sano, Y. *J. Appl. Polym. Sci.* **1993**, *50*, 107.
- (8) Okubo, M.; Shiozaki, M.; Tsujihiro, M.; Tsukuda, Y. *Colloid Polym. Sci.* **1991**, *269*, 222.
- (9) Barrett, K. E. J., Ed., *Dispersion Polymerization in Organic Media*; Wiley: London, 1975.
- (10) Almog, Y.; Reich, S.; Levy, M. *Br. Polym. J.* **1982**, *14*, 131.
- (11) Tseng, C. M.; Lu, Y. Y.; El-Aasser, M. S.; Vanderhoff, J. W. *J. Polym. Sci., Part A: Polym. Chem.* **1986**, *24*, 2995.
- (12) Tseng, C. M.; Lu, Y. Y.; El-Aasser, M. S.; Vanderhoff, J. W. *Polym. Mater. Sci. Eng.* **1986**, *54*, 362.
- (13) Ober, C. K.; Lok, K. P. *Macromolecules* **1987**, *20*, 268.
- (14) Williamson, B.; Lukas R.; Winnik, M. A.; Croucher, M. D. *J. Colloid Interface Sci.* **1987**, *119*, 559.
- (15) Paine, A. J.; McNulty, J. *J. Polym. Sci., Part A: Polym. Chem.* **1990**, *28*, 2569.
- (16) Kobayashi, S.; Uyama, H.; Yamamoto, I.; Matsumoto, Y. *Polym. J.* **1990**, *22*, 759.
- (17) Chen, Y.; Yang, H. W. *J. Polym. Sci., Part A: Polym. Chem.* **1992**, *30*, 2765.
- (18) Kobayashi, S.; Uyama, H.; Matsumoto, Y.; Yamamoto, I. *Makromol. Chem.* **1992**, *193*, 2355.
- (19) Kobayashi, K.; Senna, M. *J. Appl. Polym. Sci.* **1992**, *46*, 27.
- (20) Shen, S.; Sudol, E. D.; El-Aasser, M. S. *J. Polym. Sci., Part A: Polym. Chem.* **1993**, *31*, 1393.
- (21) Li, K.; Stöver, H. D. H. *J. Polym. Sci., Part A: Polym. Chem.* **1993**, *31*, 2473.
- (22) Tuncel, A.; Kahraman, R.; Piskin, E. *J. Appl. Polym. Sci.* **1993**, *50*, 303.
- (23) Uyama, H.; Kato, H.; Kobayashi, S. *Chem. Lett.* **1993**, 261.
- (24) Shen, S.; Sudol, E. D.; El-Aasser, M. S. *J. Polym. Sci., Part A: Polym. Chem.* **1994**, *32*, 1087.
- (25) Yabuuchi, N. *Polym. Prepr.* **1994**, *35*, 807.
- (26) Uyama, H.; Kato, H.; Kobayashi, S. *Polym. J.* **1994**, *26*, 858.
- (27) Thomson, B.; Rudin, A.; Lajoie, G. *J. Polym. Sci., Part A: Polym. Chem.* **1995**, *33*, 345.
- (28) Sáenz, J. M.; Asua, J. M. *J. Polym. Sci., Part A: Polym. Chem.* **1995**, *33*, 1511.
- (29) Horák, D.; Svec, F.; Fréchet, J. M. J. *J. Polym. Sci., Part A: Polym. Chem.* **1995**, *33*, 2329.
- (30) Horák, D.; Svec, F.; Fréchet, J. M. J. *J. Polym. Sci., Part A: Polym. Chem.* **1995**, *33*, 2961.
- (31) Hu, R.; Dimonie, V. L.; Sudol, E. D.; El-Aasser, M. S. *J. Appl. Polym. Sci.* **1995**, *55*, 1411.
- (32) Sáenz, J. M.; Asua, J. M. *J. Polym. Sci., Part A: Polym. Chem.* **1996**, *34*, 1977.
- (33) Bamnolker, H.; Margel, S. *J. Polym. Sci., Part A: Polym. Chem.* **1996**, *34*, 1857.
- (34) Baines, F. L.; Dionisio, S.; Billingham, N. C.; Armes, S. P. *Macromolecules* **1996**, *29*, 3096.
- (35) Barrett, K. E. J.; Thomas, H. R. *J. Polym. Sci., Polym. Chem. Ed.* **1969**, *7*, 2621.
- (36) Barrett, K. E. J.; Thomas, H. R.; Tolman, R. J. *IUPAC Int. Symp. Macromol. Chem.* **1969**, *3*, 369.
- (37) Ober, C. K.; Hair, M. L. *J. Polym. Sci. Part A: Polym. Chem.* **1987**, *25*, 1395.
- (38) Lok, K. P.; Ober, C. K. *Can. J. Chem.* **1985**, *63*, 209.

- (39) Ober, C. K.; Lok, K. P.; Hair, M. L. *J. Polym. Sci. Polym. Lett. Ed.* **1985**, *23*, 103.
- (40) Ober, C. K.; Van Grunsven, F.; McGrath, M.; Hair, M. L. *Colloids Surf.* **1986**, *21*, 347.
- (41) Lu, Y. Y. Ph.D. Thesis, Lehigh University, 1988.
- (42) Nilsen, T. N. Ph.D. Thesis, University of Trondheim, Norway, 1988.
- (43) Lu, Y. Y.; El-Aasser, M. S.; Vanderhoff, J. W. *J. Polym. Sci., Part B: Polym. Phys.* **1988**, *26*, 1187.
- (44) Okubo, M.; Ikegami, K.; Yamamoto, Y. *Colloid Polym. Sci.* **1989**, *267*, 193.
- (45) Paine, A. J.; Luymes, W.; McNulty, J. *Macromolecules* **1990**, *23*, 3104.
- (46) Tuncel, A.; Kahraman, R.; Piskin, E. *J. Appl. Polym. Sci.* **1994**, *51*, 1485.
- (47) Uyama, H.; Kobayashi, S. *Polym. Int.* **1994**, *34*, 339.
- (48) Kargupta, K.; Rai, P.; Kumar, A. *J. Appl. Polym. Sci.* **1993**, *49*, 1309.
- (49) Ahmed, S. F.; Poehlein, G. W. *Ind. Eng. Chem. Res.* **1997**, *36*, 2597.
- (50) Ahmed, S. F.; Poehlein, G. W. *Ind. Eng. Chem. Res.* **1997**, *36*, 2605.
- (51) van Herk, A. M. In *Polymeric Dispersions: Principles and Applications*; Asua, J. M., Ed.; Kluwer Academic Publishers: Dordrecht, The Netherlands, 1997.
- (52) Brandup, J.; Immergut, E. H., Eds. *Polymer Handbook*, 2nd ed.; Wiley: New York, 1989.
- (53) Friis, N.; Hamielec, A. E. In *Emulsion Polymerization*; Piirma, I.; Gardon, J. L., Eds.; ACS Symposium Series 24; American Chemical Society: Washington, DC, 1976.

MA980128P